Special Edition

Computational model validation of the rolled shapes calendering process

Validação de modelo computacional do processo de calandragem de perfis laminados

Mauricio da Silva Moreira[I] [ID] **, João Henrique Corrêa de Souza[I]** [ID] **,
Carlos Eduardo Marcos Guilherme[I], Liércio André Isoldi[I]** [ID]

[I]Universidade Federal do Rio Grande, Rio Grande, RS, Brasil

ABSTRACT

This paper presents the validation of computational model for the numerical simulating of the 3-roll calendering process. For this, a case study was carried out, considering a rolled I-form S235 steel profile subjected to vertical loads imposed by the calender rolls. Residual stress results obtained numerically were compared with experimental results found in the literature. The computational model was developed in ANSYS® software, which relies on the Finite Element Method (FEM), considering four different types of three-dimensional finite elements: SOLID185, SOLID186, SOLID187, and SOLID285. The results indicated that the computational model with SOLID186 presented stable mesh convergence, obtaining a discrepancy of -1.61% when compared to the experimental results, thus validating the proposed computational model.

Keywords: Mechanical forming; Numerical simulation; Finite element method

RESUMO

Este artigo apresenta a validação de modelo computacional para a simulação numérica do processo de calandragem de 3 rolos. Para isso, foi realizado um estudo de caso, considerando um perfil laminado de aço S235 em formato I submetido a esforços verticais impostos pelos rolos da calandra. Os resultados para a tensão residual, obtidos numericamente, foram comparados com resultados experimentais encontrados na literatura. O modelo computacional foi desenvolvido no software ANSYS®, que é baseado no Método dos Elementos Finitos (MEF), considerando quatro tipos diferentes de elementos finitos tridimensionais: SOLID185, SOLID186, SOLID187 e SOLID285. Os resultados indicaram que o modelo computacional com o SOLID186 obteve convergência de malha estável, com uma discrepância de -1,61% quando comparado com os resultados experimentais, validando o modelo computacional proposto.

Palavras-chave: Conformação mecânica; Simulação numérica; Método dos elementos finitos

1 INTRODUCTION

Cold-formed steel structural elements are invariably constituted by profiles with thin-walled sections of high slenderness, a characteristic that makes them highly susceptible to geometrically nonlinear effects, namely those associated to the occurrence of local, distortional or global instability phenomena (by bending or flexion-torsion). In order to properly evaluate the structural efficiency of a given structural element (profile) of cold-formed steel, it is fundamental to know its stability and post-buckling behaviors. In the last decades, the advances in the area of computational solid mechanics have allowed the use of methods and techniques of numerical analysis in structural engineering, with emphasis on the Finite Element Method (FEM) (Camotim, 2008).

Among the existing research on this topic, it is possible to highlight the study of Yang and Shima (1988) who performed a numerical simulation of the deformation of a metal profile with U-shaped cross section in a 3-roll bending (or calendering) process. The curvature distribution and bending moment were discussed according to the displacement and rotation of the rollers, and the relationship between the position of the rollers and the final curvature of the structure was reported. Some experiments of the roll bending process were performed on a 3-roll bending machine and the results obtained numerically were compared with the experimental results to confirm the accuracy of the simulation.

Spoorenberg; Snijder; Hoenderkamp, (2010) applied the method of constraints to perform the static analysis of an I-beam via finite elements. Cases were numerically simulated for different bend radii of the I-shaped rolled profile in order to obtain the residual process stresses. In these analysestwo types of finite elements were used in ANSYS® software, SOLID45 and SOLID95, to model half of the geometry through a symmetry boundary condition. For the validation of this numerical model, experimental data obtained by the authors were used.

Ktari et al. (2012) studied various parameters of 3-roll bending processes, including: the position of the upper roller, the distance between the lower rollers, and the thickness of the sheet metal. A two-dimensional finite element model was developed in the ABAQUS/Explicit environment. An industrial experiment was performed using optimized numerical results to validate the numerical model. Residual stress and plastic strain were estimated through the thickness of the work piece. The evolution of the initial bending radius versus the obtained radius was established by numerical simulation of the rolling process to obtain the elastic return. The elastic feedback obtained was compared with an analytical solution.

In Thanasoulas and Gantes (2020) the membrane residual stress and strains of roll-bent steel members comprising circular hollow sections (CHS) were examined. Detailed finite element models were developed to reliably simulate the bending procedure of CHS parts by implicit analysis accounting for geometric, contact, and material nonlinearities. Mesh convergence was followed by the parametric study in order to evaluate the influence of the main bending characteristics caused by the rollers on the developed stress/strain distributions; being these parameters: the CHS diameter and thickness, bending radius, steel yield strength, bending length, bending roller diameter, and bending die encapsulation angle. The results indicated variations in the residual stress formations, attributed to the presence of shear and transverse stresses in the CHS workpiece within the three-point bending length. The obtained residual stress distributions were summarized, and a characteristic distribution was proposed based on the plastic strains that are most commonly encountered.

In this context, the present paper employs a computational model developed in the ANSYS® software, which is based on the FEM, to numerically simulate the experiment performed by Spoorenberg; Snijder; Hoenderkamp, (2010). To do so, four types of three-dimensional finite elements were evaluated, SOLID185, SOLID186, SOLID187 and SOLID285, aiming to identify which of them is the most suitable for the numerical simulation of the calendering process.

2 METHODOLOGY

In this section a brief description of the rolled profile calendering process is presented, and the parameters used for developing the computational model and performing the numerical simulation are defined.

2.1 Calendering process for bending rolled profiles

A typical pyramid type bending machine consists of three rolls: two fixed outer rolls and a moving roller in between, as shown in Fig. 1. The movement of the middle roller produces the curvature in the profile between the two fixed rolls. In addition, the rolling of these three rolls induces a permanent curvature of the profile section as it passes above the middle roll.

Figure 1 – Pyramid type fold
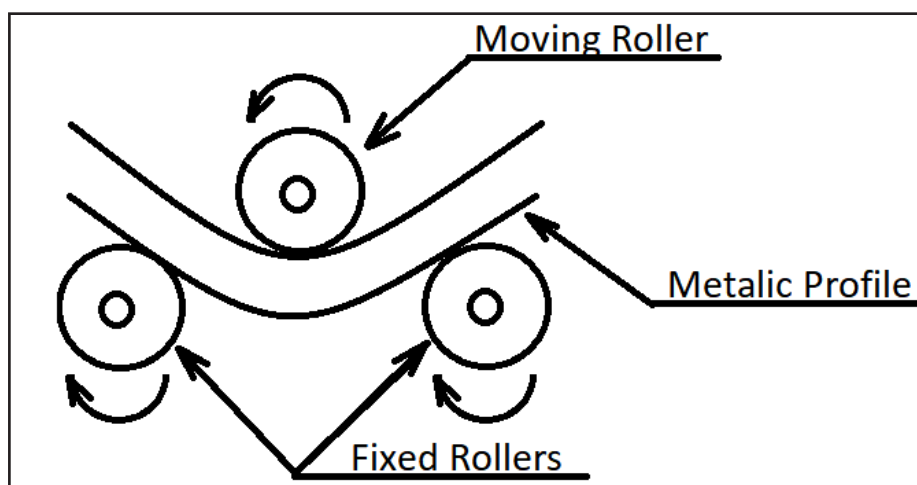
Source: Authors (August/2022)

The use of steel structures in Brazil has been constantly growing, showing that it is an efficient structural system with its own characteristics, in which the speed and organization are the main advantages of pre-industrialized systems (David, 2003).

The steel profiles used to manufacture structures are divided into three groups: rolled profiles, welded profiles, and folded sheet profiles (cold-formed profiles). The

first two can be applied in various segments of civil construction, industry, shipbuilding and foundations (David, 2003). According to Pinho (2008), parallel flange rolled profiles are the most economical for use in steel structures, to the detriment of welded profiles, which must be made to order. A relative disadvantage of rolled profiles is that they have standardized dimensions, while in welded profiles there is greater flexibility regarding the dimensions. However, if there is a concern with standardization and modulation in projects, this less flexibility of rolled profiles can be seen as an advantage. In addition, another important aspect regarding the use of rolled profiles is that the influence of residual stress in a curved member is more important than those in a straight member (King, 2001).

2.2 ANSYS software

Structural analysis is one of the most common applications of FEM. Within this context, there are several computer programs with the proposal of using this numerical method to solve a wide range of engineering problems. In the analyses performed in this paper, the ANSYS® Mechanical software was used. The structural analyses available in this program include static (linear and nonlinear), modal, spectral, dynamic, and buckling analyses. In all these analyses, the primary variables calculated are the nodal displacements, while the other quantities such as strains, stresses and reaction forces are obtained from these displacement values previously obtained for the entire computational domain (Ansys, 2022).

2.3 Finite Element Method (FEM) and description of the computational model

Zienkiewcz (1971) and Bathe (1996) summarize the finite element analysis in four steps: geometry creation (computational domain), mesh generation (discretization of the computational domain into elementary parts), application of the boundary conditions and external loading, and finally the problem solution.

The computational model developed for the numerical simulation of the

I-profile calendering processes considers geometric and material nonlinearities as well as surface-to-surface contact effects. The consideration of geometric and contact nonlinearity is necessary due to the large deformations and because the horizontal displacement of the profile occurs through friction existing on the contact surfaces along with the rotation of the rollers. The material behavior was approximated by a multilinear relationship. The true stress and strain values considered for the numerical simulation were taken from experimental tests performed by Spoorenberg; Snijder; Hoenderkamp, (2010). Regarding the behavior of the materials, the rolls were adopted as rigid while the I-profile was considered as flexible, since the calender rolls have stiffness higher than that of the rolled profile material. For the purpose of reducing processing time, the beam and rollers were modeled with only half of their profiles, being adopted a symmetry boundary condition through a plane that is located in the middle of the beam web thickness (see Fig. 2). A right roller displacement of 53 mm in the vertical direction was adopted, thus promoting a bending radius of 1910 mm in profile I, as in Spoorenberg; Snijder; Hoenderkamp, (2010).

The augmented Lagrangian algorithm was selected, the constraint (boundary conditions) is satisfied through Lagrange multipliers, thus omitting the use of high penalty stiffness, avoiding convergence difficulties and poor conditioning of the global stiffness matrix. This, however, is at the cost of more equilibrium iterations compared to other algorithms (Ansys, 2022).

Figure 2 – Dimensions of half of the rolled I-profile and the rolling rolls (in mm)
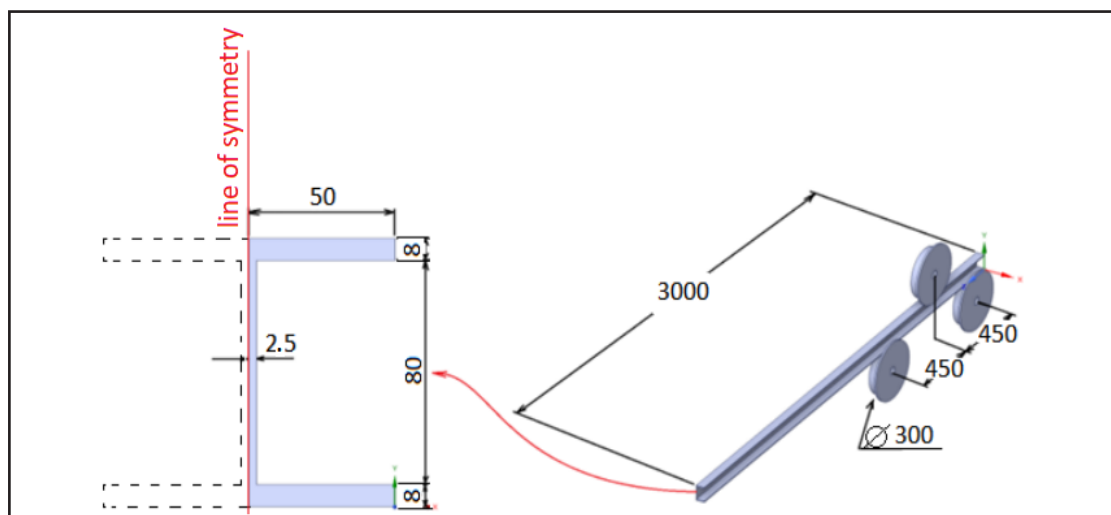
Source: Authors (August/2022)

2.4 Types of finite elements used

Different 3D finite elements (SOLID185, SOLID186, SOLID187 and SOLID285) were tested to model the I-profile in order to evaluate which one would obtain better results compared to the experimental data of Spoorenberg et al. (2010); while the CONTA174 element was used to model the contact surfaces on the I-profile, promoting the contact between the I-profile and the rolling rolls. The contact element is located on the surfaces of the SOLID element, and the arrangement of the nodes conforms to it. On the other hand, the TARGE170 element was adopted for the rollers: when the CONTA174 elements of the I-profile contact surface penetrate the TARGE170 elements, the contact is established.

The SOLID185 element is a suitable option for general 3D modeling of solid structures, allowing prismatic, tetrahedral, and pyramidal degenerations in irregular regions. It has eight nodes with three degrees of freedom at each node, being translations in the nodal x, y, and z directions. It is capable of plasticity, hyperelasticity, strain hardening, creep, large deflection, and large deformation capacity. Moreover, it has mixed formulation capabilities to simulate deformations of nearly incompressible elastoplastic materials and fully incompressible hyperelastic materials (BNE, 2017).

SOLID186 is a higher-order 3D solid element defined by 20 nodes with three degrees of freedom per node that supports plasticity, hyperelasticity, creep, stress stiffening, large deflection, and large strain capacity (BNE, 2017).

SOLID187, another higher order element, is also suitable for irregular meshes, having 10 nodes with three degrees of freedom at each node, and has the same capabilities as SOLID185 and SOLID186 (BNE, 2017).

SOLID285 is a mixed 4-node 3D lower order uP element with linear displacement and hydrostatic pressure behavior, and is capable of simulating deformations of nearly incompressible elastoplastic materials, nearly incompressible hyperelastic materials, and totally incompressible hyperelastic materials (BNE, 2017).

The CONTA174 element is used to represent the contact and sliding between surfaces in 3D structural contact and coupled field analysis. It can be used for both pair-based contact and general contact. In the case of pair-based contact, the target surface is defined by the 3D target element type, TARGE170. In the case of general contact, the target surface can be defined by CONTA174 elements for deformable surfaces (I-beam) or TARGE170 elements that are used only for rigid bodies (calender rollers) (BME, 2017).

The finite elements considered in the developed computational model and described above can be seen in Fig. 3.

Figure 3 – shows the finite elements used in the paper to computationally model the 3-roll bending forming process applied to an I-profile
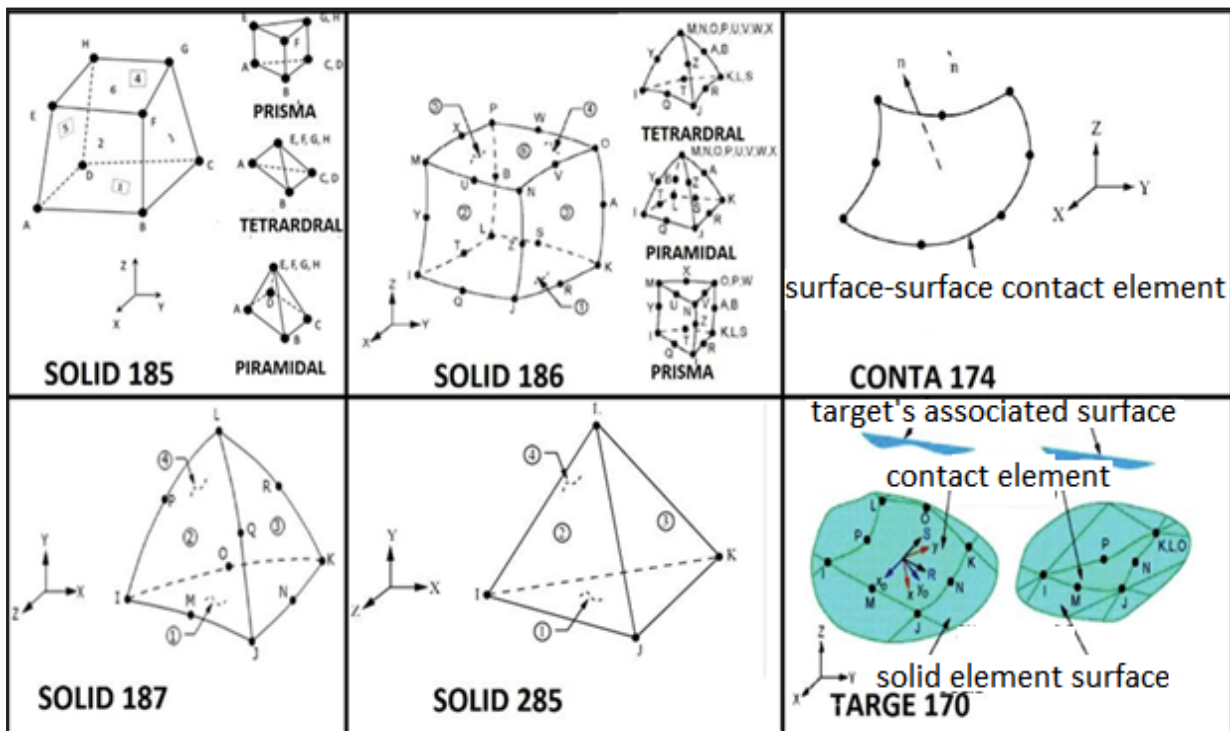
Source: ANSYS (2022)
Note: adapted image

3 RESULTS AND DISCUSSIONS

Initially, it was carried out a mesh convergence test for each type of 3D finite element considered. After that, the experiment presented in Spoorenberg et al. (2010) was numerically simulated with the 3D finite element indicated by the mesh convergence test, aiming to promote the computational model validation.

3.1 Mesh convergence test

The mesh convergence test was performed in order to evaluate if the numerical results are independent of the adopted spatial discretization. Therefore, the ideal mesh size is sought to find the best relationship between accuracy and computational cost, i.e., when the obtained results vary minimally in relation to the mesh refinement.

The student version of ANSYS® 2022 software was used, having a limit of 128,000 nodes for structural analysis. Therefore, the mesh convergence test was done respecting this limitation.

As a parameter for the mesh convergence test the maximum tensile stress in the I-profile flange was adopted, based on the experimental results of Spoorenberg; Snijder; Hoenderkamp, (2010). It should be noted that all stresses compared in this work are on the external surface of the rolled profile, since the experimental data of the stresses at this location are presented in a more complete way in Spoorenberg; Snijder; Hoenderkamp, (2010).

From the results of the mesh convergence test presented in Table 1, a mesh with 6033 SOLID186 finite elements was selected as ideal for the computational modeling of the problem, which obtained a maximum tensile stress of 347.91 MPa. It was observed that SOLID186 was the only finite element that showed convergent results, reaching a relative difference between two successive refinements of less than 1%.

Table 1 – Mesh convergence test

Finite Element	Number of Finite Elements	Maximum Tensile Stress (MPa)	Relative Difference (%)	Processing Time
SOLID185	3789	186.57	-18.44	01 h 01 min
SOLID185	5513	220.97	-38.22	02 h 14 min
SOLID185	6423	305.43	30.15	03 h 03 min
SOLID185	8700	213.34	-4.63	03 h 30 min
SOLID185	9483	223.23	54.53	04 h 07 min
SOLID185	10533	101.49	-	04 h 22 min
SOLID186	2562	307.99	-6.66	01 h 22 min
SOLID186	3615	328.50	-2.61	03 h 47 min
SOLID186	4731	337.09	-2.02	05 h 40 min
SOLID186	5321	343.90	-1.17	07 h 11 min
SOLID186	6033	347.91	-0.61	08 h 53 min
SOLID186	7383	350.02	-	10 h 51 min
SOLID187	14510	283.32	-3.39	02 h 43 min
SOLID187	16525	292.94	-1.31	03 h 57 min
SOLID187	18618	296.77	-6.77	04 h 52 min
SOLID187	20377	316.87	8.94	05 h 28 min
SOLID187	24277	288.54	6.59	08 h 11 min
SOLID187	30027	269.53	-	10 h 52 min
SOLID285	13550	230.55	-5.93	00 h 35 min
SOLID285	16712	244.22	-4.23	01 h 55 min
SOLID285	18245	254.55	-2.23	02 h 23 min
SOLID285	21002	260.22	12.05	03 h 45 min
SOLID285	23995	228.85	17.19	04 h 51 min
SOLID285	30021	189.50	-	05 h 30 min

Source: authors (2022)

3.2 Numerical simulation results with SOLID186

In Figure 4 it is possible to analyze the quality of the spatial discretization generated when using the converged mesh with the SOLID186 finite element and 6033 elements. The color scale on the left side of Fig. 4 defines the quality of each generated finite element in the computational domain, ranging on a scale between 0 (bad finite element) and 1 (perfect finite element).

According to the ANSYS®, the quality of the mesh structure element is

calculated by:

$$Quality \ = \ C \left[\frac{volume}{\sqrt{[\sum(edge\ length)^2]^3}}\right]$$

(1)

This equation is valid for 3D mesh elements in ANSYS®. The parameters are the same for 2D and 3D meshing elements; volume and edge length. The constant C in Eq. (1) varies depending on the type of element used.

Figure 4 – Mesh obtained with SOLID186 finite element
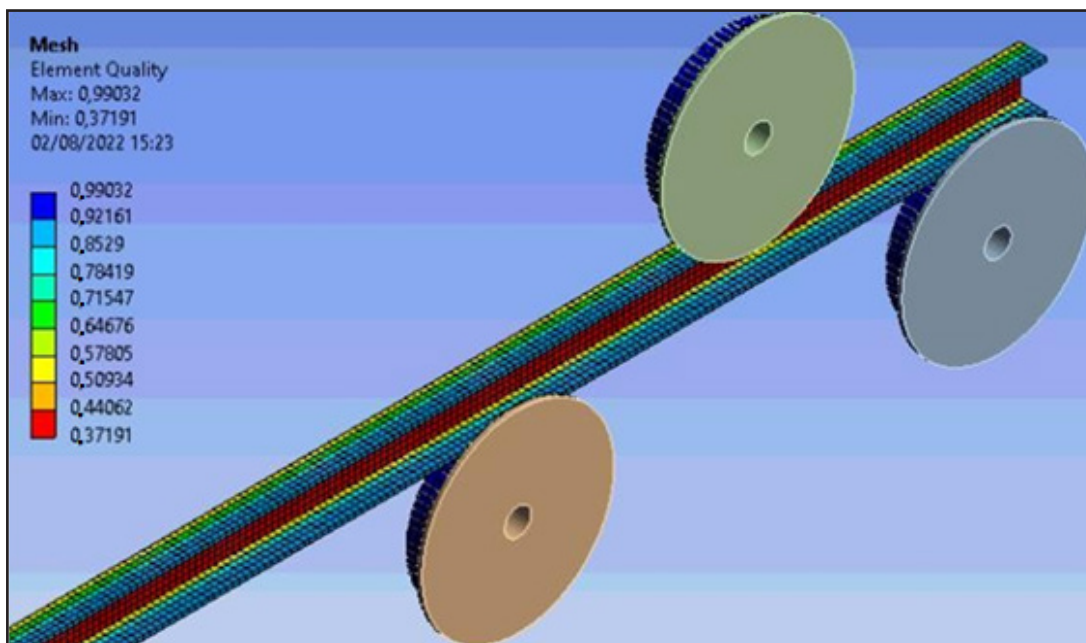
Source: Authors (August/2022)

Figure 5 shows the von-Mises stresses resulting from the forming process numerically simulated. However, to perform the comparison with the experimental results it was necessary to obtain the residual stresses of the process, i.e., the elastic stresses existing in a body without the existence of external loads or temperature gradients. To do so, three paths were created in the geometry after the unloading forces. These paths allowed obtaining the numerical simulation results only in these specific regions.

Figure 5 – The von-Mises stresses distribution numerically obtained
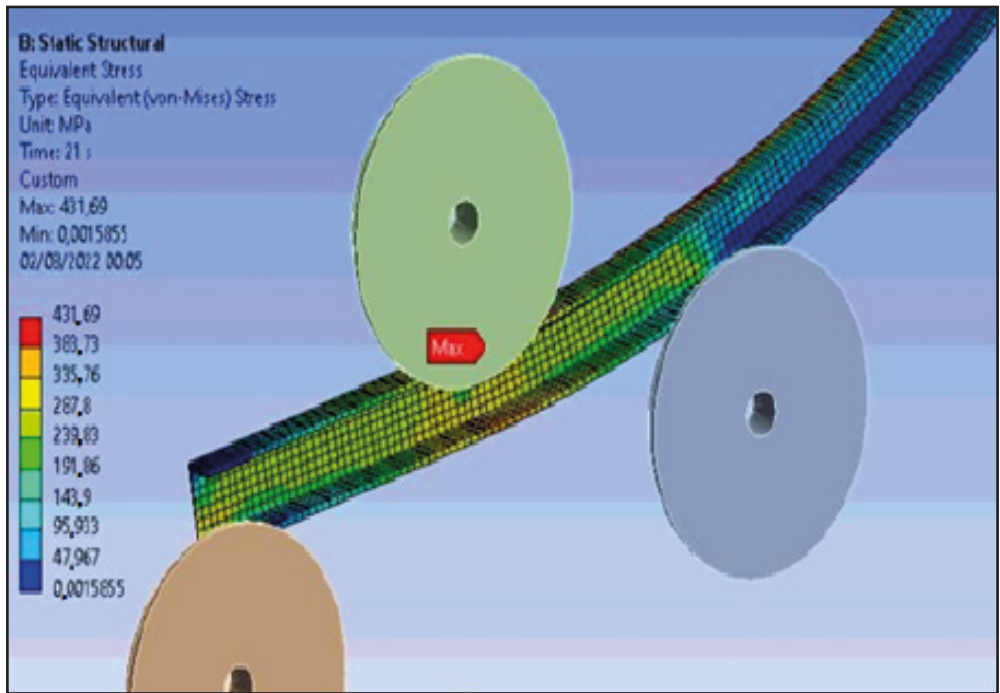
Source: Authors (August/2022)

Figure 6 – The residual stresses variantion in the: (a) upper flange, (b) lower flange, and (c) web of the beam
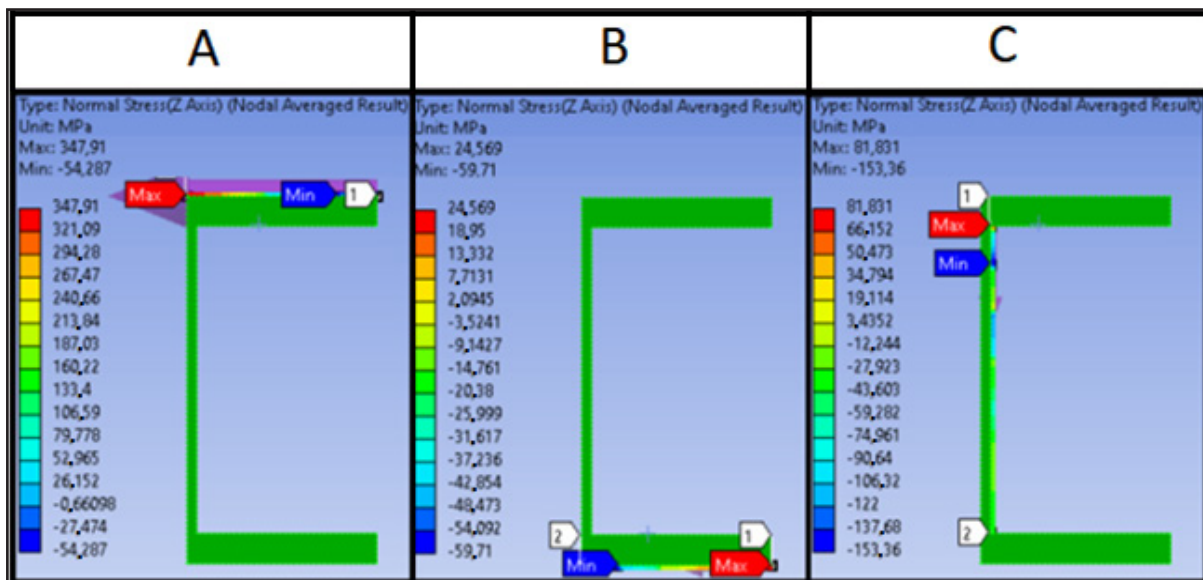
Source: Authors (August/2022)

In Figure 6, one can see the residual stresses along the paths located at the: upper flange (Fig. 6a), lower flange (Fig. 6b), and web of the beam (Fig. 6c). The results presented in Fig. 6 showed a variation of the residual stresses ranging between -153.36 MPa e 347.91 MPa. It can be seen from these results that the maximum tensile stress is in the upper flange of the beam while the maximum compressive stress is in the web.

Finally, considering the stresses obtained in the numerical simulation it was possible to make a comparison of these results with the experimental ones from Spoorenberg; Snijder; Hoenderkamp (2010), as shown in Fig. 7.

Figura 7 – comparação dos resultados numéricos e experimentais
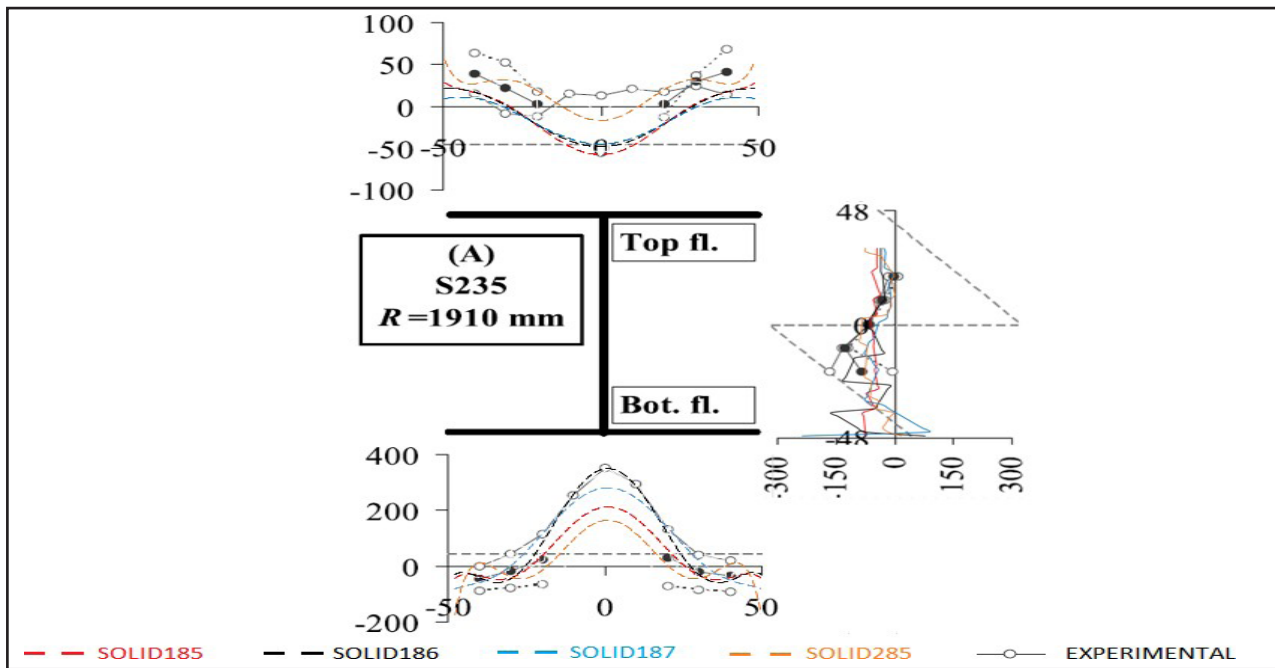
Source: Authors (August/2022)

As can be seen in Fig. 7 the numerical results had a good approximation to the experimental ones. The region that presented a lower accuracy was the core of the I-profile, however, even so, there was a good agreement and a moderate accuracy in relation to the experimental results. The results presented a discrepancy of approximately -1.61% when compared with the maximum experimental stress value (353.6 MPa), thus validating the developed model.

4 CONCLUSIONS

It can be observed that the four computational models developed presented the same trend in relation to the profile of forces developed along the profile, but only the model that used the SOLID186 finite element had a greater approximation in terms of absolute value. It is concluded that the computational modeling performed with the SOLID186 finite element presents results compatible with the published scientific references, therefore, the methodology used in this study proves to be useful for obtaining results of residual stresses in an I-profile with a discrepancy of - 1.61%. The difference in accuracy in the results of the flanges in relation to the web of the beam can be explained by the difficulty of generating higher quality elements in this area, as seen in Fig. 4.

In future work, it is intended to use the numerical model developed and validated here for studies of different profiles.

ACKNOWLEDGEMENTS

REFERENCES

Ansys Inc. (2022), A*NSYS User's Manua*l: Analysis Systems.

Bathe, K. J. *Finite Element Procedures*. Prentice Hall. 1996

BME - *Budapest University of Technology and Economics*, 2017. Available from: https://www.mm.bme.hu/~gyebro/files/ans_help_v182/ans_elem/. Accessed on: 15 Apr. 2022.

Camotim, D.; Silvestre, N.; Dinis, P. B. Análise numérica de elementos estruturais de aço enformados a frio: desenvolvimentos recentes e perspectivas futuras. *Revista Sul-Americana de Engenharia Estrutural.* 2008.

David, D. L. Vigas mistas com laje treliçada e perfis formados a frio: análise do comportamento estrutural. 2003. Dissertação (Mestrado em engenharia civil), Universidade Federal de Goiás, Goiânia, 2003.

King, C. e Brown, D. *Design of Curved Steel*. 2001. The Steel Construction Institute, Berkshire.

Ktari, A.; Antar, Z.; Haddar, N.; Elleuch, K. Modeling and computation of the three-roller bending process of steel sheets. 2012. *Journal of Mechanical Science and Technology*, 26 (1), 123-128.

Pinho, F. O. Quando construir em aço? 2008. *Revista Engenharia*, ed. 593.

Spoorenberg, R. C.; Snijder, H. H.; Hoenderkamp, J. C. D. Finite element simulations of residual stresses in roller bent wide flange sections. 2010. *Journal of Constructional Steel Research,* 67, 737 – 747.

Thanasoulas, I. D.; Gantes, C. J. Numerical investigation on the residual stresses of roller-bent circularhollow-sections. 2020. *Journal of Constructional Steel Research*, 164.

Yang, M.; Shima, S. Simulation of pyramid type three-roll bending process International. 1988. *Journal of Mechanical Science*, 30, 877 – 886.

Zienkiewicz, O. C. *The finite Element Method.* 1971. in Engineering Science, 2ª ed., McGraw- Hill, London.

Authorship contributions

1 – Mauricio da Silva Moreira

G.Eng., Universidade Federal do Rio Grande
https://orcid.org/0000-0002-7945-048X -mauriciodsm6@gmail.com
Contribution: Conceptualization, Data curation, Investigation, Methodology, Software, Validation, Writing – original draft

2 – João Henrique Corrêa de Souza

Dr. Ing., Institute of Metal Forming Technologies
https://orcid.org/0000-0002-5181-0201 - joaohenrique@technnova.com.br.
Contribution: Methodology, Resources, Supervision, Visualization, Writing – review & editing

3 – Carlos Eduardo Marcos Guilherme

Dr. Eng., Universidade Federal do Rio Grande do Sul
http://lattes.cnpq.br/7137044566348475 - carlosguilherme@furg.br.
Contribution: Formal analysis, Funding acquisition, Project administration, Supervision, Methodology, Writing – review & editing

4 – Liércio André Isoldi

Dr. Eng., Universidade Federal do Rio Grande do Sul.
https://orcid.org/0000-0002-9337-3169 - liercioisoldi@furg.br.
Contribution: Data curation, Formal analysis, Funding Acquisition, Investigation, Methodology, Project administration, Resources, Supervision, Validation, Visualization, Writing – review & editing

How to quote this article